First-principles study of optical properties of barium titanate

Cite as: Appl. Phys. Lett. **83**, 2805 (2003); https://doi.org/10.1063/1.1616631
Submitted: 06 May 2003 . Accepted: 16 August 2003 . Published Online: 30 September 2003

Meng-Qiu Cai, Zhen Yin, and Ming-Sheng Zhang

First-principles study of optical properties of barium titanate

Meng-Qiu Cai, Zhen Yin,[a] and Ming-Sheng Zhang
National Laboratory of Solid State Microstructures and Department of Physics, Nanjing University, Nanjing 210093, China

(Received 6 May 2003; accepted 16 August 2003)

The optical properties of perovskite barium titanate in the core-level spectra are investigated by the first principles under scissor approximation. There are nine peaks at the curve of the imaginary part of dielectric function. The optical spectra are assigned to interband contribution from O $2p$ valence bands to Ti $3d$ conduction bands in the low-energy region and outer core electron excitation (core level excitation) from near valence band semicore levels Ba $5p$ and O $2s$ to conduction band in the high-energy region. In contrast to the calculated results by the tight-binding linear muffin-tin orbitals method, our results are in better agreement with the experimental results. © *2003 American Institute of Physics.* [DOI: 10.1063/1.1616631]

Barium titanate ($BaTiO_3$) as a typical perovskite material has been attractive for its fundamental research interest and perspective applications in the fields of ferroelectricity, microelectronics and optoelectrics, as micro-capacitors, microsensors, optical switches, and so on.[1–3] With respect to experimental study, Spitzer *et al.* measured the infrared reflectivity spectra of $BaTiO_3$ in a low-energy range and obtained principal dielectric functions via Kramers–Kronig relations.[4] Jona *et al.* studied the structural, dielectric, elastic, and thermal properties.[5] Bäuerle *et al.* measured the infrared reflectivity spectra of in a high-energy range and obtained the several optical constants.[6] Moreover, Mara *et al.* and Cardona *et al.* investigated the infrared and the Raman as well as electron-spin resonance spectra, respectively.[7–11] With regard to theoretical study, Saha *et al.* calculated optical properties of $BaTiO_3$ by the tight-binding linear muffin-tin orbitals (TB-LMTO) method within the atomic-sphere approximation.[12] Their results were fair agreement with the experimental data in the low-energy range below 10 eV, but the results above 10 eV were not given. Thus, there has not been a comparison between theoretical and experimental results in the high-energy spectra, and their origin is still not clear.

In this letter, we have calculated and investigated the optical properties of paraelectric $BaTiO_3$ up to 0–30 eV by using an accurate full-potential, linearized, augmented plane-wave method under the scissor approximation technique (FLAPW-SAT).[13,14] The local-orbital basis functions were implemented in the latest WIEN2K code.[15,16] Exchange and correlation effects are treated within the generalized gradient approximation (GGA).[17] The underestimation for the band gap by GGA was corrected by SAT,[14] which amounts to a rigid shift of the conduction band (CB) states so that the experimentally reported gap is well reproduced.

It is known that the dielectric function is mainly connected with the electronic response. The imaginary part $\epsilon_2(\omega)$ of the dielectric function $\epsilon(\omega)$ is calculated from the momentum matrix elements between the occupied and unoccupied wave functions and given by

$$\epsilon_2(\omega)=\frac{ve^2}{2\pi\hbar m^2\omega^2}\int d^3k\sum_{m,n'} B_{m,n'}|\langle \mathbf{k}n|\mathbf{p}|\mathbf{k}n''\rangle|^2 \times f(\mathbf{k}n)(1-f(\mathbf{k}n'))\,\delta(E_{\mathbf{k}n}-E_{\mathbf{k}n'}-\hbar\omega),$$

where $\hbar\omega$ is the energy of the incident phonon, $\mathbf{p}$ is the momentum operator, $(\hbar/i)$, $(\partial/\partial x)$, $|\mathbf{k}n\rangle$ is a crystal wave function, and $f(\mathbf{k}_n)$ is the Fermi function. The real part $\epsilon_1(\omega)$ of dielectric function $\epsilon(\omega)$ is evaluated from imaginary part $\epsilon_2(\omega)$ by the Kramer–Kronig transformation. All other optical constants on the energy dependence of absorption coefficient $I(\omega)$, refractive index $n(\omega)$, extinction coefficient $k(\omega)$, energy-loss spectrum $L(\omega)$, and reflectivity $R(\omega)$ can be derived from $\epsilon_1(\omega)$ and $\epsilon_2(\omega)$.[12]

The paraelectric phase of $BaTiO_3$ belongs to cubic structure with a space group $Pm3m$ (O_h^1), with the Ba atom sitting at the origin point, the Ti at the body centers, and the three oxygen atoms at the three face centers.[5] The muffin-tin sphere radii are R_i=2.0, 1.8, and 1.5 a.u. for Ba, Ti, and O atoms, respectively. For controlling the size of basis set for the wave functions, $R_{\mathrm{mt}}K_{\max}$ was set to 7.0, and the well-converged basis sets consist of about 775 LAPW functions and 36 local orbits chosen for O $2s$, Ti $3p$, Ti $3d$, and Ba $5p$ states. Integrations in the reciprocal space were performed by using the tetrahedron method and a $12\times12\times12$ mesh was used to represent 51 k-points in the irreducible wedge of Brillouin zone (BZ). The spin–orbit coupling was not taken into in our calculation since it has a minor influence on the optical properties for ferroelectricity and semiconductor materials.[18,19]

Shown in Fig. 1 is the calculated band structure along the high-symmetry directions in the BZ. Nine valence bands (VBs) between 0 and −4.5 eV consist of O $2p$ orbitals, which is consistent with results by x-ray photoemission spectroscopy.[7] The nine valence bands at the Γ of the center of the BZ are the three triply degenerate level $^1\Gamma_{15}$, Γ_{25}, and $^2\Gamma_{15}$, for which the values of the energy are −2.31, −1.58, and −0.16 eV, respectively. Below O $2p$ bands, Ba $5p$ and O $2s$ orbitals form the narrow semicore bands. The three bands at $^3\Gamma_{15}$ (about −9.88 eV) are derived from Ba $5p$ orbitals, and at $^1\Gamma_1$ (about −16.89 eV) and $^2\Gamma_1$ (about

[a]Electronic mail: zyin@nju.edu.cn

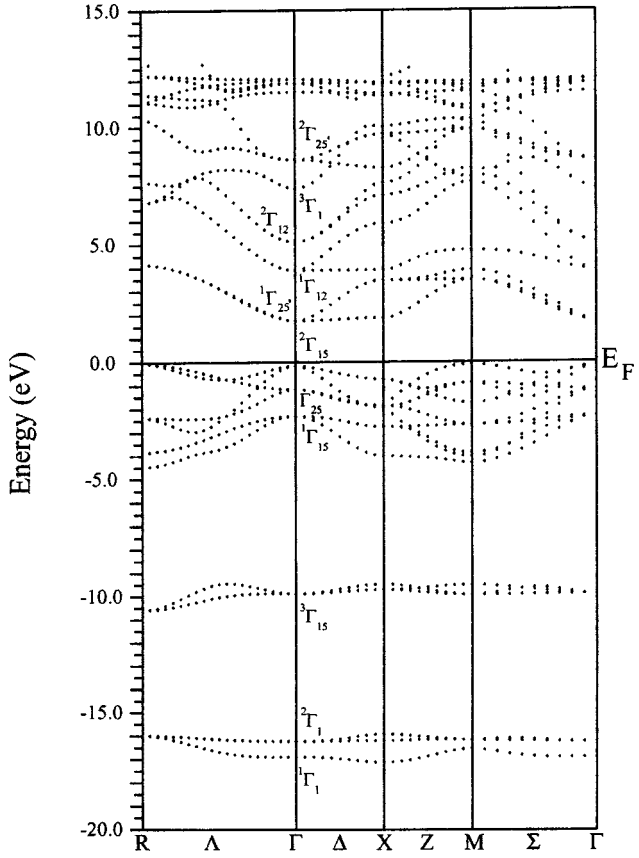

FIG. 1. The calculated energy band structure of $BaTiO_3$ along the high-symmetry directions in the BZ.

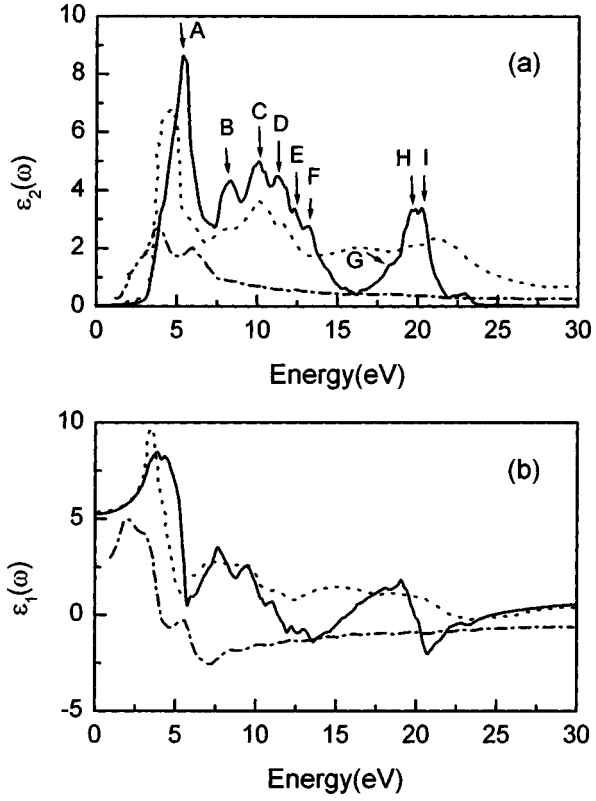

FIG. 2. (a) the imaginary part $\epsilon_2(\omega)$ and (b) real part $\epsilon_1(\omega)$ of the dielectric function $\epsilon(\omega)$ of the paraelectric $BaTiO_3$ as a function of the photon energy. The dotted lines represent experimental data (Ref. 6), the dash-dot lines and solid lines represent theoretically calculated results by TB-LMTO (Ref. 12) and FLAPW-SAT, respectively.

-16.22 eV), they are derived from O $2s$ orbitals. The states at the bottom of CB arise from the threefold degenerate Ti $3d\,T_{2g}$ orbitals between around 1.76 and 4.5 eV, which have lower energy than the twofold degenerate Ti $3d\,E_g$ orbitals between about 4.0 and 8.0 eV. The Ti $3d$ energy bands at Γ point are $^1\Gamma_25'$ (about 1.76 eV) and $^1\Gamma_{12}$ (about 3.91 eV). Between about 6.0 and 12 eV, the dispersive bands are high-energy CB Ba $6s$ and Ba $5d$, and these bands at Γ point are $^2\Gamma_{12}$ (about 5.12 eV), $^3\Gamma_1$ (about 7.42 eV), and $^2\Gamma_{25'}$ (about 8.62 eV). Moreover, a direct band gap is 1.918 eV at the center of the BZ Γ point, which is much closer to the experimental value (3.2 eV)[8] than the calculated value of band gap (1.2 eV) using the TB-LMTO method.[12]

The $\epsilon_2(\omega)$ and $\epsilon_1(\omega)$ as a function of the photon energy are shown in Figs. 2(a) and 2(b), respectively, where the dot lines represent experimental data (Ref. 6), the dash-dot lines and solid lines stand for the results calculated by TB-LMTO method (Ref. 12) and our FLAPW-SAT method, respectively. The scissor approximation operator make a rigid shift 1.28 eV of CB toward higher energies to reproduce the experimental band gap 3.2 eV to compensate for this systematic error of the local density approximation. The assignments of the critical peaks in the optical spectra of $\epsilon_2(\omega)$ in Fig. 2(a) are as follows. Peaks A (5.35 eV) and B (8.30 eV) correspond mainly to the transition from O $2p$ VB to Ti $3d$ CB, and peaks C (10.05 eV), D (11.26 eV), E (12.32 eV), and F (13.32 eV) correspond mainly to the transitions from O $2p$ VB to Ba $6s$ and Ba $5d$ high-energy CB. The corresponding experimental peaks in points E and F are not apparent. There are no clean-cut structures for $\epsilon_2(\omega)$ above 16 eV, because the oscillator strengths coupling between the VB and CB vanish.[20] The optical properties of critical peaks of G (18.22 eV), H (19.85 eV), and I (20.03 eV) are ascribed to the transitions of inner electron excitation from near VB semicore states Ba $5p$ and O $2s$ levels to CB, which is consistent with the experimental prediction.[6] It is noted that a peak in $\epsilon_2(\omega)$ does not correspond to a single interband transition since many direct or indirect transitions may be found in the band structure with an energy corresponding to the same peak.

Our calculated $\epsilon_2(\omega)$ by FLAPW-SAT is in good agreement with the experimental result,[6] much better than those calculated results by TB-LMTO method, where only two major peaks are at about 3.8 and 5.9 eV and the two peaks showed energy differences of 1.0 and 4.0 eV, respectively.[12] Our full-potential, linearized, augmented plane-wave method did not make shape approximation, and the core states were calculated self-consistently in the crystal potential, leading to obtaining the right dielectric functions.

Figures 3(a)–3(e) show the calculated results on the energy dependence of absorption coefficient $I(\omega)$, refractive index $n(\omega)$, extinction coefficient $k(\omega)$, energy-loss spectrum $L(\omega)$, and reflectivity $R(\omega)$, respectively. For the $I(\omega)$ calculation, we consider only the eigen-absorption, without considering the polarized absorption, which has minor influence on $I(\omega)$.[21] The absorption coefficient is very large (about 10^6 cm^{-1}) and decreases rapidly in the low-energy region. The function $L(\omega)$ shown in Fig. 3(d) describes the energy loss of a fast electron traversing the material.[22] The

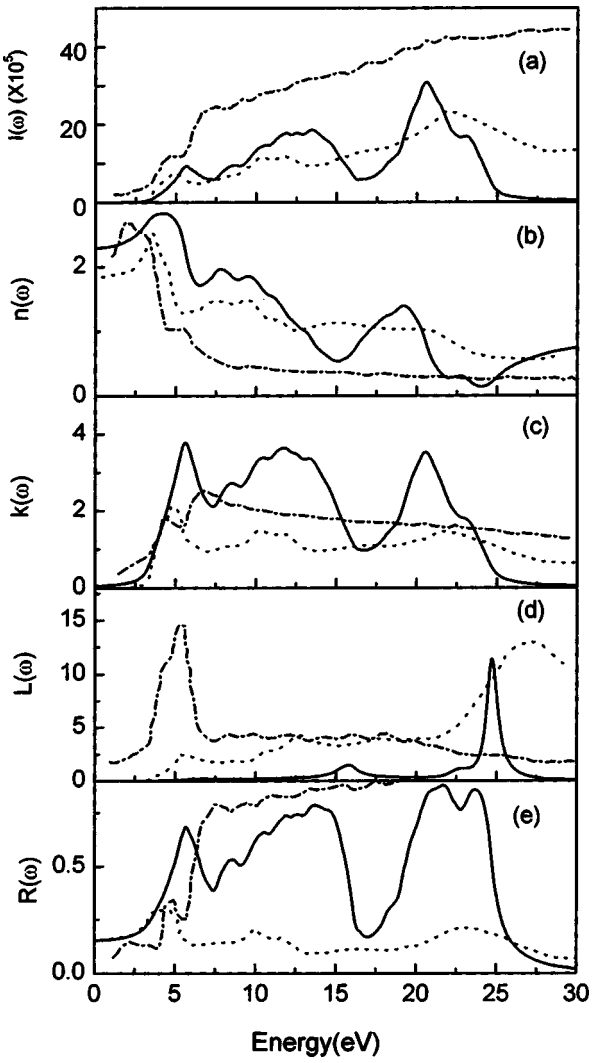

FIG. 3. The calculated optical parameters of the $BaTiO_3$ as a function of the photon energy eV. $I(\omega)$ (a), $n(\omega)$ (b), $k(\omega)$ (c), $L(\omega)$ (d), and $R(\omega)$ (e) stand for absorption coefficient, refractive index, extinction coefficient, energy-loss spectrum, and reflectivity, respectively. The dotted lines stand for experimental data (Ref. 6), the dash-dot lines and solid lines denote calculated results by TB-LMTO (Ref. 12) and FLAPW-SAT, respectively.

sharp peak is associated with the plasma oscillation.[23] The peak of the $L(\omega)$ spectrum calculated by our FLAPW-SAT is at 25 eV, which is in excellent agreement with experimental results of 27 eV,[6] much better than the value of 5 eV calculated by TB-LMTO.[12] It should be pointed out that such a large discrepancy of $L(\omega)$ stemmed from plasma excitation. The calculated $\epsilon_1(\omega)$ by TB-LMTO equals zero at about 5 eV, but our calculated $\epsilon_1(\omega)$ by FLAPW equals zero at about 18 eV, as shown in Fig. 2(b). The sharp structure at about 25 eV in our calculated $L(\omega)$ spectrum corresponds to a rapid decrease of reflectance in Fig. 3(e). This process is associated with transitions from the filled Ba $5p$ and O $2s$ bands, lying below the VB, to an empty CB. From the earlier description, our calculated optical constants of $I(\omega)$, $n(\omega)$, $k(\omega)$, $L(\omega)$, and $R(\omega)$ are in good agreement with the experimental data[6] in the wide-energy ranges. However, the calculated results by the TB-LMTO method,[12] only approximately reproduced some of low-energy optical properties and could not match the experimental results in the high-energy region. These discrepancies could arise from the noticeable difference between their dielectric functions by the TB-LMTO method and the experimental ones.

In summary, we have calculated electronic band structure and optical properties of $BaTiO_3$ using the FLAPW-SAT method in a wide energy range. Our calculated results show that the complex dielectric function and the energy-dependent optical constants such as $I(\omega)$, $n(\omega)$, $k(\omega)$, $L(\omega)$, and $R(\omega)$ are also in good agreement with the experimental data in the low- and high-energy regions. The properties of optical spectra of $BaTiO_3$ are assigned to the contribution of interband transition from valence band O $2p$ levels to conduction band Ti $3d$ levels or even higher conduction band Ba $6s$ and $5d$ in the low-energy region, and to outer core electron excitation from near valence band semicore states Ba $5p$ and O $2s$ to Ti $3d$ conduction band in the high-energy region.

This work has been supported by the National Natural Science Foundation of China through Grant 10174034 and the Natural Science Foundation of Jiangsu Province through Grant BK2001026. The authors would express their thanks to the Supercomputer Center of Nanjing University for computation support. The calculation was performed at computer SGI Origin 3800 under WIEN2K code.

[1] R. Migoni, H. Bilz, and D. Bauderle, Phys. Rev. Lett. **37**, 1155 (1976).
[2] G. Binnig and H. E. Hoenig, Solid State Commun. **14**, 597 (1974).
[3] E. R. Pfeiffer and J. F. Schooley, J. Low Temp. Phys. **2**, 333 (1970).
[4] W. G. Spitzer, R. C. Miller, D. A. Kleinman, and L. E. Howarth, Phys. Rev. **126**, 170 (1962).
[5] F. Jona and G. Shirane, *Ferroelectrics Crystals* (Macmillan, New York, 1962).
[6] D. Bäuerle, E. Braun, V. Saile, G. Sppussel, and E. E. Kock, Z. Phys. B **29**, 179 (1978).
[7] P. Pertosa, G. Hollinger, and F. M. Michel-Calendini, Phys. Rev. B **18**, 5177 (1978).
[8] R. T. Mara, G. B. B. Sutherland, and H. V. Tyrell, Phys. Rev. **96**, 801 (1954).
[9] M. Cardona, Phys. Rev. **140**, A651 (1965).
[10] S. H. Wemple, Phys. Rev. B **2**, 2679 (1970).
[11] R. Scharfschwerdt, A. Mazur, O. F. Schirmer, H. Hesse, and S. Mendricks, Phys. Rev. B **54**, 15284 (1996).
[12] S. Saha and T. P. Sinha, Phys. Rev. B **62**, 8828 (2000).
[13] D. J. Singh, *Planewaves, Pseudopotentials and LAPW Method* (Kluwer Academic, Boston, 1994).
[14] Z. H. Levine and D. C. Allan, Phys. Rev. B **43**, 4187 (1991).
[15] D. J. Singh, Phys. Rev. B **43**, 6388 (1991).
[16] P. Blaha, K. Schwarz, G. K. H. Madsen, D. Kvasnicka, and J. Luitz, *WIEN2K* (Technical University of Vienna, Austria, 2001), ISBN 3-9501031-1-2.
[17] J. P. Perdew, K. Burke, and M. Ernzerhof, Phys. Rev. Lett. **77**, 3865 (1996).
[18] S. Sharma, C. Ambrosch-Draxl, P. Blaha, and S. Auluck, Phys. Rev. B **60**, 8610 (1999).
[19] R. Ahuja, O. Eriksson, B. Johansson, and J. M. Wills, Phys. Rev. B **54**, 10419 (1996).
[20] S. Kohiki, Phys. Rev. B **57**, 14572 (1998).
[21] C. Persson, R. Ahuja, A. Ferreira da Silva, and B. Johansson, J. Cryst. Growth **231**, 407 (2001).
[22] P. Nozieres, Phys. Rev. Lett. **8**, 1 (1959).
[23] L. Marton, Rev. Mod. Phys. **28**, 172 (1956).